DEVELOPMENTAL BIOLOGY

Molecular to organismal chirality is induced by the conserved myosin 1D

G. Lebreton[1]*, C. Géminard[1]†‡, F. Lapraz[1]‡, S. Pyrpassopoulos[2]‡, D. Cerezo[1], P. Spéder[1]§, E. M. Ostap[2], S. Noselli[1]¶

The emergence of asymmetry from an initially symmetrical state is a universal transition in nature. Living organisms show asymmetries at the molecular, cellular, tissular, and organismal level. However, whether and how multilevel asymmetries are related remains unclear. In this study, we show that *Drosophila* myosin 1D (Myo1D) and myosin 1C (Myo1C) are sufficient to generate de novo directional twisting of cells, single organs, or the whole body in opposite directions. Directionality lies in the myosins' motor domain and is swappable between Myo1D and Myo1C. In addition, Myo1D drives gliding of actin filaments in circular, counterclockwise paths in vitro. Altogether, our results reveal the molecular motor Myo1D as a chiral determinant that is sufficient to break symmetry at all biological scales through chiral interaction with the actin cytoskeleton.

Asymmetry is ubiquitous in living organisms and plays essential roles at all biological scales from molecular to behavioral (e.g., polarization of neurons, asymmetric division of stem cells, location of organs, hand preference, etc.). Chirality is a particular kind of asymmetry. A molecule or organ is said to be chiral if it is not superimposable on its mirror image, like our left and right hands.

A fundamental feature of biological systems lies in the chiral uniformity (or homochirality) of the building blocks (L-amino acids, D-sugars, chiral polymers including DNA, microtubules, F-actin, etc.) from which they are assembled. Whether macroscopic asymmetries (e.g., the location of the human heart on the left side of the body or the handedness of snail shell coiling) of living organisms are directly related to their molecular chirality remains an open question. Such a link was suggested by the "F-molecule model," involving a hypothetical F-shaped chiral molecule whose three arms would orient cells in space and differentiate left from right (*1*). The occurrence of asymmetries at all biological scales further raises the question of their origin and mode of propagation. In other words, does a single asymmetry-determining process propagate to higher levels, or do multiple independent processes occur? To understand the role of chirality in biological systems, we examined the establishment of left-right (LR) asymmetry in *Drosophila* (*2*–*5*). In this organism, the conserved *myosin 1D* (*myo1D*) gene is essential for dextral looping of all native LR organs (*6*–*9*). *myo1D* is a situs inversus gene, as its absence leads to the full reversal of organ positioning along the LR axis, with organs adopting a mirror-image orientation (referred to as sinistral). *Drosophila* has several independent, tissue-specific LR organizers in which *myo1D* is expressed and necessary (*10*–*14*).

To determine whether *myo1D* is sufficient to drive LR asymmetry, we ectopically expressed the protein in different naïve tissues (i.e., tissues devoid of LR asymmetry). We found that Myo1D expression in the larval epidermis induces dextral twisting of the whole larval body (Fig. 1, A and B). This phenotype is 100% penetrant and is specific to Myo1D (fig. S1, A to E). The larval body can rotate up to 180°, flipping the mouth parts toward the dorsal side of the larvae (Fig. 1B) and misaligning adjacent denticle belts by 17.4° [0° in wild type (WT)] (fig. S1, F, G, and I). Of note, twisted posture alters locomotion behavior: the larvae move through directional barrel rolling rather than through normal crawling (movie S1). Dextral twisting can also be induced in pupae and adult abdomens (fig. S2, A to D).

To test whether *myo1D* can induce asymmetry at the single-organ level, we ectopically expressed it in tracheal precursors. In this condition, the whole trachea undergoes pronounced dextral twisting (see materials and methods), adopting a spiraling ribbon shape with multiple turns, instead of the smooth and linear conformation of WT trachea (Fig. 1, C and D, and fig. S3). We next investigated twisting at the cellular level, through quantification of the geometry and polarity of epidermal cells expressing Myo1D ectopically. In control conditions, cell membrane orientation shows a Gaussian distribution centered on 0° [i.e., cells are perpendicular to the anterior-posterior (AP) axis] (Fig. 1E). In contrast, Myo1D-expressing cells show elongation (fig. S4) and a clear shift in membrane orientation toward one side (Fig. 1F), indicating that Myo1D also induces directional polarization at the cell level.

The Myo1D protein contains head (motor), neck, and tail domains that are all essential for normal Myo1D function (*15*). To assess their requirement for *myo1D* gain-of-function phenotypes, we expressed Myo1D proteins with point mutations or truncations (*15*). Results show that the integrity of the protein is essential, with all domains being required (Fig. 1G). Point mutations in actin- or adenosine triphosphate (ATP)–binding sites indicate that Myo1D actin-based motor activity is crucial for its function in establishing both native (*15*) and de novo LR asymmetry (Fig. 1G).

To test Myo1D specificity in generating de novo asymmetry, we ectopically expressed seven other *Drosophila* myosins (Fig. 2, A to C, and fig. S5, A to G). Only Myo1C (*16*) overexpression led to twisted larvae (Fig. 2C). Myo1C-induced twisting is opposite (sinistral) to that of Myo1D (Fig. 2, A to C) and less pronounced (90° versus 180° for Myo1D), with a denticle belt angle of −9.9° instead of 17.4° for Myo1D (fig. S1, F, H, and I). Myo1C also induces twisting of trachea (Fig. 2, E and F), pupae, and adults (fig. S2, E and F), as well as spiraling locomotion (movie S2), all with sinistral orientation. Additionally, Myo1C-expressing cells show opposite lateralized polarity to Myo1D-expressing cells (Fig. 2, G and H). Finally, Myo1C requires the same domain integrity as Myo1D for sinistral twisting (Fig. 2I), in particular a fully functional motor domain. We found that both myosins are antagonistic, cancelling out each other's gain-of-function phenotype (Fig. 2, B to D, and fig. S2, G and H), reminiscent of previous data showing that Myo1C can antagonize Myo1D in native LR organs (*6*, *17*).

The fact that two paralogous myosins can polarize the whole larvae in opposite ways provides a framework for determining the molecular basis of directionality. Thus, we performed structure-function analysis by swapping the head, neck, and tail domains from each protein (Fig. 3). Expression of each chimera in the larvae showed that the determinant for directionality in these myosins lies in their motor-head domain (Fig. 3). Keeping the neck and tail domains from the same protein increases protein activity, whereas swapping the sole neck reduces it markedly (Fig. 3), suggesting an important coupling between head and neck for full myosin activity.

Myosin head domains are known to directly interact with actin filaments. Chickadee, the *Drosophila* homolog of profilin, is involved in actin polymerization. Reducing chickadee protein expression led to the suppression or strong reduction of the body-twisting phenotypes induced by either of the myosins (fig. S6, A to G), pointing to actin formation and/or dynamics for myosin chiral activity. Next, we assessed the ability of myosins to produce motion of actin filaments while bound to fluid-supported lipid bilayers in vitro (*18*). Both myosins bind to phosphatidylinositol 4,5-bisphosphate [PI(4,5)P2] (fig. S7) and propel actin filament motility on supported lipid bilayers (movie S3), with Myo1D having a speed 1.7 times that of Myo1C (table S1). Myo1D drove counterclockwise, circular motility of actin, whereas Myo1C did not show any turning bias in these conditions (Fig. 4, A and B, and table S1). Circular motility persisted when Myo1D was attached to a fluid bilayer by means of a biotin-streptavidin linkage, confirming the finding that asymmetric motility is a property of the motor domain. Mixing the two proteins and increasing the Myo1C/Myo1D ratio reduces circular F-actin movement, thus recapitulating the Myo1C antagonism toward

[1]Université Côte D'Azur, CNRS, Inserm, Institut de Biologie Valrose, Nice, France. [2]Pennsylvania Muscle Institute and the Center for Engineering Mechanobiology, University of Pennsylvania, Perelman School of Medicine, Philadelphia, PA, USA.
*Present address: Centre de Biologie Intégrative, Université Paul Sabatier, 118 Route de Narbonne, 31062 Toulouse Cedex, France. †Present address: Institut de Recherche en Cancérologie de Montpellier (IRCM), Inserm U1194, 208 Avenue des Apothicaires, 34298 Montpellier Cedex 5, France. ‡These authors contributed equally to this work. §Present address: Institut Pasteur, 25 Rue du Dr Roux, 75015 Paris, France.
¶Corresponding author. Email: noselli@unice.fr

Myo1D observed in vivo for normal and de novo LR asymmetry (Figs. 2D and 4C) (*6*, *17*). Altogether, these results reveal a chiral interaction between Myo1D and F-actin in vitro, providing evidence for a molecular origin of LR asymmetry induced by this myosin at the cell, organ, and whole-body levels.

In conclusion, Myo1D represents a chiral determinant that is necessary for native handedness and sufficient to create de novo LR asymmetry from the molecular to the behavioral level, with chiral information being encoded within the motor domain itself. We propose that the multiscale property of Myo1D emerges from its molecular chiral interaction with F-actin (Fig. 4D). This model is in accordance with the so-called F-molecule model for LR asymmetry establishment (*1*), predicting that chiral factors (in particular, molecular motors) set axis direction at the molecular level through vector information and then propagate across organization scales.

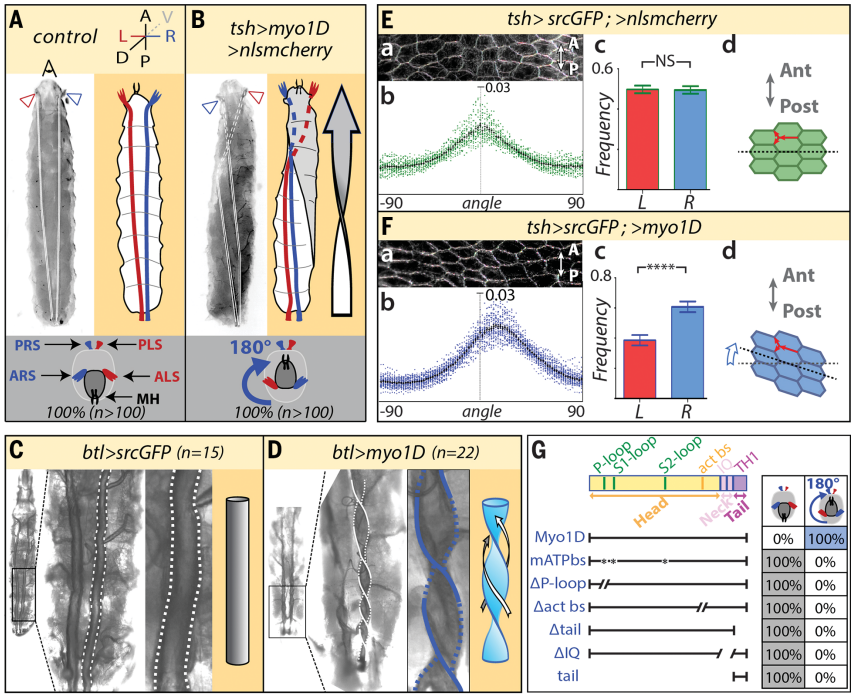

Fig. 1. Myo1D induces de novo LR asymmetry. (**A**) (Top) Control larvae (white, left panel; schematized, right panel) showing bilateral symmetry. The trachea is indicated, with anterior tracheal spiracles indicated by a red (left) or blue (right) open triangle. (Bottom) Front view of the larvae (ventral down, dorsal up). MH, mouth hooks; ALS, anterior left spiracle; ARS, anterior right spiracle; PLS, posterior left spiracle; PRS, posterior right spiracle. Left and right spiracles are shown in red and blue, respectively. A, anterior; P, posterior; L, left; R, right; D, dorsal; V, ventral. (**B**) *myo1D* expression in the epidermis (*tsh>myo1D*) is sufficient to induce dextral twisting of the whole larval body by 180°. (**C**) Linear morphology of a control (*btl>srcGFP*) third instar larvae trachea. (**D**) *myo1D* expression in the tracheae (*btl>myo1D*) induces their dextral twisting with multiple loops. (**E** and **F**) Morphometric analysis of the larval epidermis of WT (Ea) and *myo1D*-expressing epidermal cells (Fa). Graphic plot showing distribution of cellular angles relative to the AP axis (Eb and Fb) and plot of the sum of rightward (−90° to 0°:R)− against leftward (0° to 90°:L)−oriented angles (Ec and Fc), showing that *myo1D* overexpression induces polarized reorganization of epithelial cells toward the dextral orientation (Ed and Fd). *n* = 24 (*n*, sample size) for *tsh>srcGFP>nls-mCherry*; *n* = 39 for *tsh>myo1D-RNAi>srcGFP*. Error bars indicate SD. ****$P < 0.0001$; NS, nonsignificant. (**G**) Structure-function analysis of Myo1D twisting activity. Integrity of the protein as well as its ATP- and actin-binding sites are essential for its function. *n* = 25 for each.

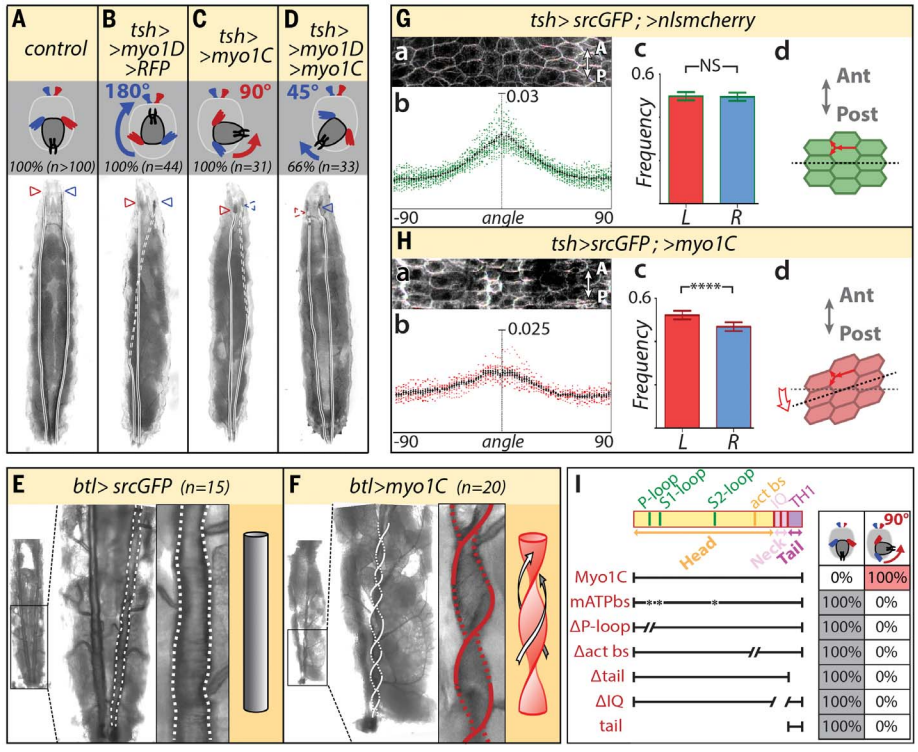

Fig. 2. Myo1C is a sinistral myosin antagonist to Myo1D. (**A** to **D**) Control (white) larvae (A) and larval-twisting phenotype induced by overexpression of *myo1D* (B) or *myo1C* (C) or by coexpression of *myo1D* and *myo1C* (D). (**E**) Linear morphology of a control (*btl>srcGFP*) third instar larvae trachea. (**F**) *myo1c* expression in the tracheae (*btl>myo1C*) induces their sinistral twisting. (**G** and **H**) Morphometric analysis of the larval epidermis of WT (Ga) and *myo1C*-expressing epidermal cells (Ha). Graphic plot showing distribution of cellular angles relative to the AP axis (Gb and Hb) and plot of the sum of rightward (−90° to 0°:R)− against leftward (0° to 90°:L)−oriented angles (Gc and Hc), showing that *myo1C* overexpression induces polarized reorganization of epithelial cells toward sinistral (Gd and Hd). *n* = 24 for *tsh>srcGFP>nls-mCherry*; *n* = 12 for *tsh>myo1C-RNAi>srcGFP*. Error bars indicate SD. ****$P < 0.0001$; NS, nonsignificant. (**I**) Structure-function analysis of Myo1C twisting activity. Integrity of the protein, as well as its ATP- and actin-binding sites, is essential for its function. *n* = 25 for each.

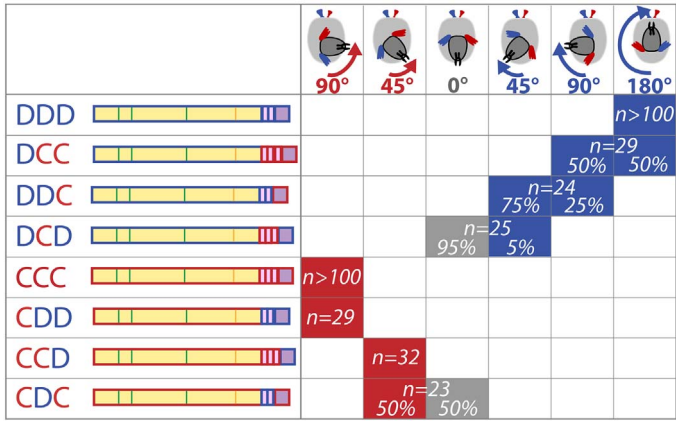

Fig. 3. The motor domain confers Myo1D and Myo1C chirality. Twisting activity of all Myo1D-Myo1C chimeras swapping head (motor), neck, and tail domains. The head domain provides directionality to the proteins. Domains designated D and C pertain to Myo1D and Myo1C, respectively.

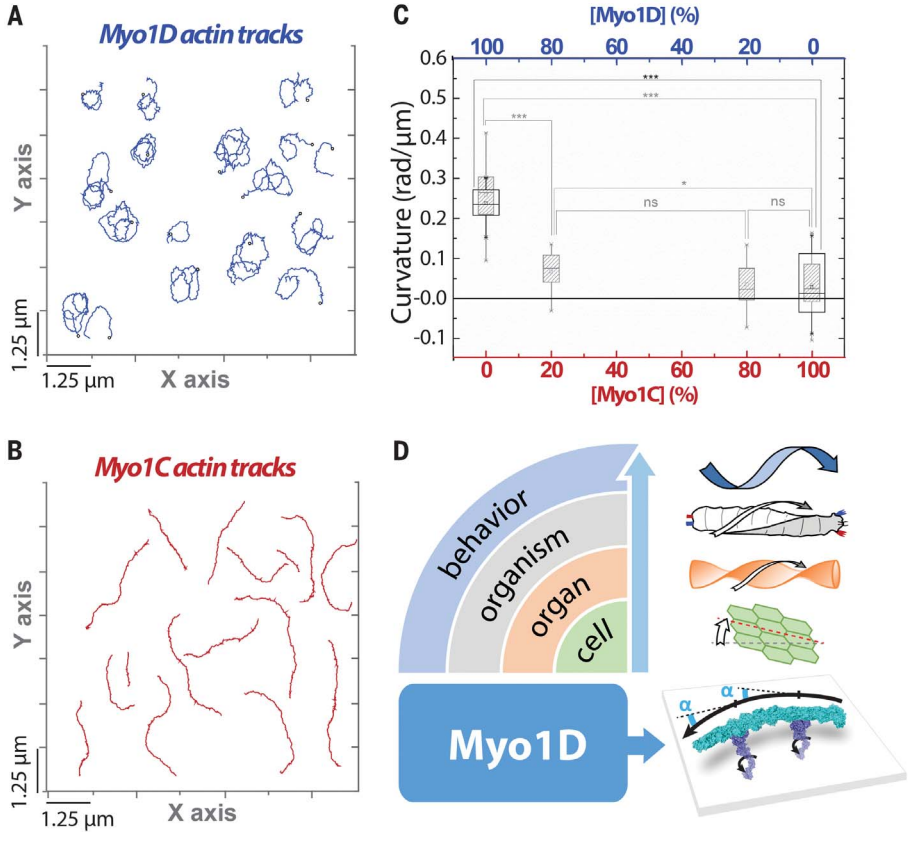

Fig. 4. Chiral interaction between Myo1D and F-actin in vitro. (**A** and **B**) Representative tracks (track origin indicated by open circle) of actin filaments from actin gliding assays on 2% PI(4,5)P2, 98% dioleoylphosphatidylcholine (DOPC)–supported lipid bilayers for Myo1D (A) and Myo1C (B). (**C**) Curvature of actin filament tracks on 2% PI(4,5)P2, 98% DOPC (black boxes)– and 2% biotinPE, 98% DOPC (gray boxes)–supported lipid bilayers for different relative Myo1D and Myo1C concentrations. Error bars correspond to the minimum and maximum values of each dataset. ***$P < 0.001$; *$P < 0.05$; ns, nonsignificant. (**D**) Model of Myo1D chiral activity across multiple organization scales. Bottom cartoon represents actin filament (cyan) gliding powered by Myo1D (purple) on lipid bilayers (gray). The black arrow indicates the actin gliding direction. For most myosins, the power stroke occurs in the direction of the actin filament axis. Mechanisms for actin turning (angle α) include (i) myosin lever-arm translation no longer along the long axis of the actin filament, (ii) myosin lever-arm circular rotation during the power stroke (arrows), or (iii) myosin-induced actin conformational change that results in leftward bending of the actin filament.

Myo1D's ability to generate de novo asymmetry has two important meanings. First, it indicates that some tissues are competent for asymmetry but lack chiral determinant activity, with Myo1D exposing an intrinsic yet only partly unfolded polarized LR axis. Second, the large-scale changes in organ and/or body shape and in posture and/or behavior triggered by simple misregulation of Myo1D fit the fundamental property of so-called toolkit genes proposed to control morphological evolution (*19*). Hence, our findings provide clues to understand the origin of torsion in evolution, proposed to rely on a single genetic event (macromutation) for a gastropod's 180° torsion (*20*). Accordingly, recent results have shown the essential role of actin regulators in snail coiling (*21*, *22*).

REFERENCES AND NOTES

1. N. A. Brown, L. Wolpert, *Development* **109**, 1–9 (1990).
2. M. Blum, K. Feistel, T. Thumberger, A. Schweickert, *Development* **141**, 1603–1613 (2014).
3. J.-B. Coutelis, N. González-Morales, C. Géminard, S. Noselli, *EMBO Rep.* **15**, 926–937 (2014).
4. T. Nakamura, H. Hamada, *Development* **139**, 3257–3262 (2012).
5. A. Raya, J. C. Izpisúa Belmonte, *Nat. Rev. Genet.* **7**, 283–293 (2006).
6. S. Hozumi *et al.*, *Nature* **440**, 798–802 (2006).
7. P. Spéder, G. Adám, S. Noselli, *Nature* **440**, 803–807 (2006).
8. M. Tingler *et al.*, *Curr. Biol.* **28**, 810–816.e3 (2018).
9. T. Juan *et al.*, *Nat. Commun.* **9**, 1942 (2018).
10. J. B. Coutelis, A. G. Petzoldt, P. Spéder, M. Suzanne, S. Noselli, *Semin. Cell Dev. Biol.* **19**, 252–262 (2008).
11. C. Géminard, N. González-Morales, J. B. Coutelis, S. Noselli, *Genesis* **52**, 471–480 (2014).
12. P. Spéder, S. Noselli, *Curr. Opin. Cell Biol.* **19**, 82–87 (2007).
13. N. González-Morales *et al.*, *Dev. Cell* **33**, 675–689 (2015).
14. M. Suzanne *et al.*, *Curr. Biol.* **20**, 1773–1778 (2010).
15. S. Hozumi *et al.*, *Dev. Dyn.* **237**, 3528–3537 (2008).
16. N. S. Morgan, D. M. Skovronsky, S. Artavanis-Tsakonas, M. S. Mooseker, *J. Mol. Biol.* **239**, 347–356 (1994).
17. A. G. Petzoldt *et al.*, *Development* **139**, 1874–1884 (2012).
18. S. Pyrpassopoulos, E. A. Feeser, J. N. Mazerik, M. J. Tyska, E. M. Ostap, *Curr. Biol.* **22**, 1688–1692 (2012).
19. S. B. Carroll, *Cell* **134**, 25–36 (2008).
20. W. F. Ponder, D. R. Lindberg, *Zool. J. Linn. Soc.* **119**, 83–265 (1997).
21. R. Kuroda *et al.*, *Sci. Rep.* **6**, 34809 (2016).
22. A. Davison *et al.*, *Curr. Biol.* **26**, 654–660 (2016).

ACKNOWLEDGMENTS

We thank K. Matsuno, J. Casanova, and T. Lin for reagents; the Bloomington *Drosophila* Stock Center, the National Institute of Genetics Fly (NIG-Fly), and Vienna *Drosophila* RNAi Center (VDRC) for providing *Drosophila* fly lines; the iBV PRISM platform; M. Gettings (Getting Published) for comments; and members of the S.N. laboratory for discussions. **Funding:** F.L. is supported by Agence Nationale pour la Recherche (ANR; ANR-13-BSV2-0006) and Université Côte d'Azur (UCA); G.L. is supported by ANR (ANR-13-BSV2-0006). E.M.O. is supported by NIH Grant R37GM057247. Work in the S.N. laboratory is supported by ANR (ANR-13-BSV2-0006; ANR-17-CE13-0024), UCA, Centre National pour la Recherche Scientifique (CNRS), Institut National pour la Recherche Médicale (Inserm), and the LABEX SIGNALIFE (ANR-11-LABX-0028-01). **Author contributions:** G.L. and S.N. designed the experiments. G.L., C.G., and F.L. performed the experiments (except gliding assays), with the help of D.C. P.S. constructed the chimeras. S.P. performed and S.P. and E.M.O. designed and analyzed the gliding assays. G.L., E.M.O., and S.N. wrote the manuscript with input from all of the authors. **Competing interests:** Authors declare no competing interests. **Data and materials availability:** All data are available in the main text or the supplementary materials.

SUPPLEMENTARY MATERIALS

www.sciencemag.org/content/362/6417/949/suppl/DC1
Materials and Methods
Figs. S1 to S7
Table S1
References (*23*–*30*)
Movies S1 to S3

13 April 2018; accepted 4 October 2018
10.1126/science.aat8642

Science

Molecular to organismal chirality is induced by the conserved myosin 1D

G. Lebreton, C. Géminard, F. Lapraz, S. Pyrpassopoulos, D. Cerezo, P. Spéder, E. M. Ostap and S. Noselli

Science **362** (6417), 949-952.
DOI: 10.1126/science.aat8642

A single myosin sets chirality at all scales

When viewed externally, most organisms appear symmetric between the left and right sides. However, many organs are left-right asymmetric. Whether macroscopic asymmetries are directly related to molecular-level chirality remains an open question. Working in *Drosophila*, Lebreton *et al.* found that the conserved molecular motor myosin 1D induced stereotyped chirality at all biological scales—from F-actin turning in vitro to the organ level and even organismal behavior. Thus, a single conserved myosin can generate de novo nano-to-macroscopic changes in form and direction through chiral interaction with the actin cytoskeleton.

Science, this issue p. 949